Electronic Supplementary Material (ESI) for CrystEngComm.

Electronic Supporting Information

Unidirectional Growth of Single Crystalline β-$Na_{0.33}V_2O_5$ and α-V_2O_5 Nanowires Driven by Controlling of pH in Aqueous Solution and Their Electrochemical Performances for Na-Ion Batteries

Yejung Lee,[a,d] Seung Mi Oh,[a,d] Boyeon Park,[a] Byeong Uk Ye,[b] Nam-Suk Lee,[c] Jeong Min Baik,[b] Seong-Ju Hwang,[a,*] and Myung Hwa Kim[a,*]

[a] Department of Chemistry & Nanoscience, Ewha Womans University, Seoul, 120-750, Korea

[b] *School of Mechanical and Advanced Materials Engineering, KIST-UNIST-Ulsan Center for Convergent Materials, Ulsan National Institute of Science and Technology (UNIST), Ulsan, 689-798, Korea*

[c] *National Institute for Nanomaterials Technology (NINT), Pohang University of Science and Technology (POSTECH), Pohang, 790-784, Korea*

[d] *Authors contributed equally to this work.*

[*] To whom all correspondence should be addressed: myungkim@ewha.ac.kr, hwangsju@ewha.ac.kr

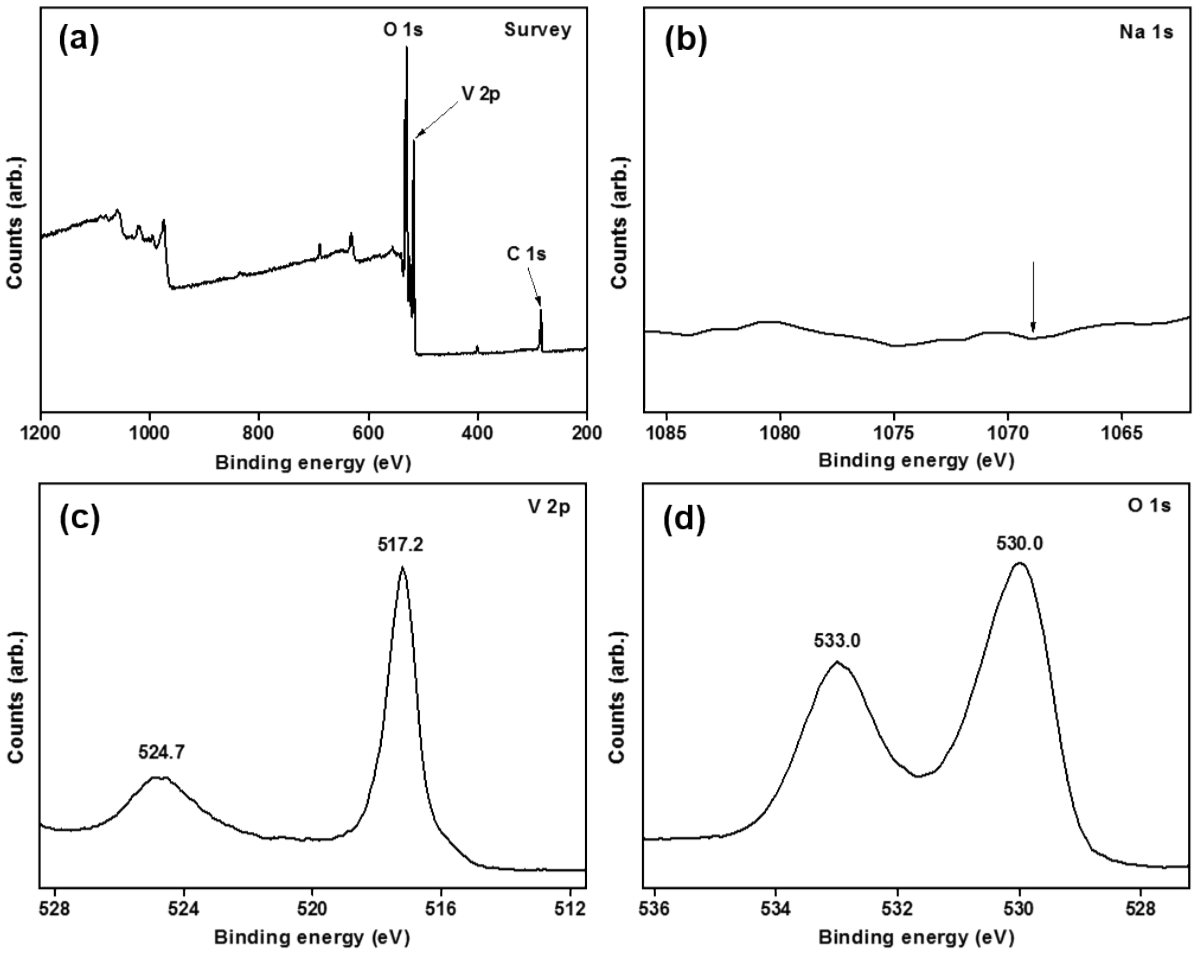

Fig. S1 Low and high-resolution X-ray photoelectron spectra (XPS) of as-grown V_2O_5 nanowires on a Si substrate at 500 °C. (a) Survey spectrum, (b) Na 1s, (c) V 2p, and (d) O 1s regions of as grown V_2O_5 nanowires.

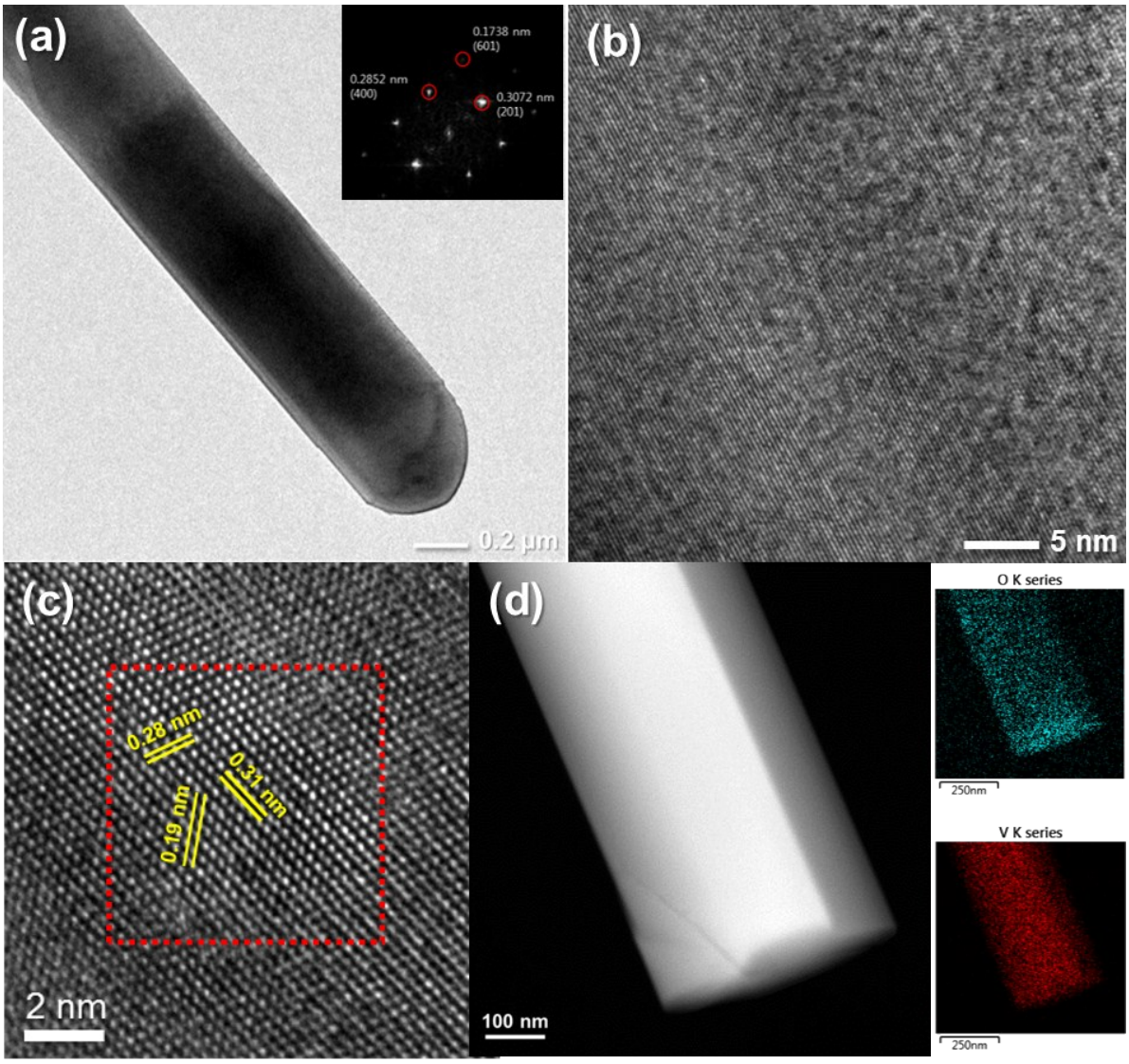

Fig. S2 (a, b) Low and high magnification transmission electron microscopy (TEM) image and inset (b) shows the Fast Fourier Transform (FFT) of the lattice resolved image. (c) the lattice resolved high resolution transmission electron microscopy (HRTEM) image of a single V_2O_5 nanowire. (d) High angle annular dark field (HAADF) scanning transmission electron microscopy (STEM) image of a single V_2O_5 nanowire and energy dispersive spectrometry (EDS)-elemental mapping analysis for V(K) and O(K) atoms of a single V_2O_5 nanowire.

Table S1. Parameters obtained by fitting analyses for Nyquist plots on the basis of the Voigt-type equivalent circuit.

Samples	R_s (Ω)	R_f (Ω)	R_{ct} (Ω)
β-$Na_{033}V_2O_5$ nanowire	13.06	3.706	16.03
α-V_2O_5 nanowire	6.67	2.981	18.92

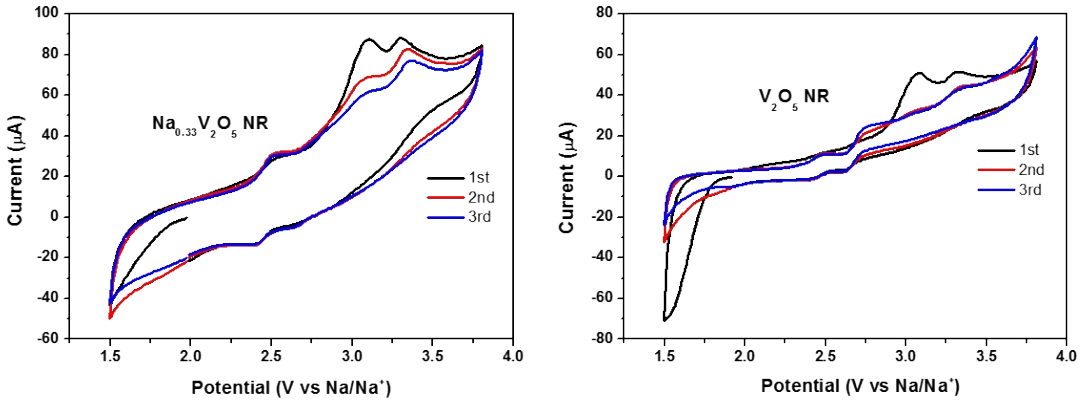

Fig. S3 CV profiles of β-$Na_{0.33}V_2O_5$ nanowires and α-V_2O_5 nanowires measured at scan rate of 0.1 mV s^{-1}.

For the detailed analysis for the electrochemical redox reaction occurring in the present vanadium oxide electrodes, the CV curves of these materials were measured. As illustrated in Fig. S3, β-$Na_{0.33}V_2O_5$ nanowire has two reduction peaks at 2.4 and 2.6 V as well as two oxidation peaks at 2.5, 3.1, and 3.3 V. These redox peaks are assigned as the reduction/oxidation of vanadium ion caused by the multi-step insertion/desertion of Na^+ ion. Similarly, α-V_2O_5 nanowire displays two reduction peaks at 2.4 and 2.6 V, and four oxidation peaks at 2.5, 2.7, 3.1, and 3.3 V, which are related to the redox process of vanadium ion. The CV area and peak intensity are greater for the β-$Na_{0.33}V_2O_5$ nanowire than for the α-V_2O_5 one, clearly demonstrating the fast electrochemical kinetics of the former material.

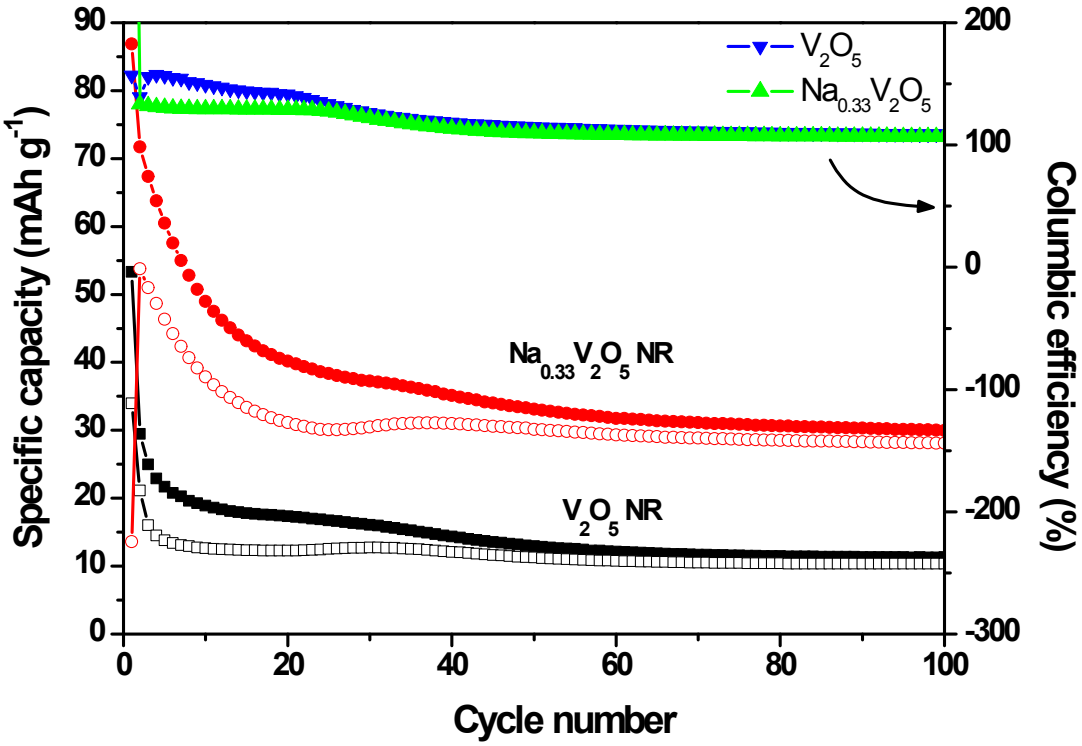

Fig. S4 Plots of charge/discharge capacities and Coulombic efficiencies vs. cycle number for β-$Na_{0.33}V_2O_5$ nanowires and α-V_2O_5 nanowires measured at current density of 80 mA g^{-1}.

The charge and discharge capacities of the β-$Na_{0.33}V_2O_5$ nanowires and α-V_2O_5 nanowires measured are also measured at current density of 80 mA g^{-1}. As plotted in Fig. S4, β-$Na_{0.33}V_2O_5$ nanowire also delivers greater discharge capacities than does the α-V_2O_5 nanowire, confirming the better SIB electrode performance of the former. The coulombic efficiency (CE) is also calculated to understand the electrochemical desodiation/sodiation process occurring in the present vanadium oxides. Both the β-$Na_{0.33}V_2O_5$ and α-V_2O_5 nanowires exhibit unusually high CE of ≥100%, implying greater charge capacity than the corresponding discharge capacity. Such an unusually high CE is already reported for other vanadium oxide, which is attributable to the decomposition of electrolyte and the dissolution of vanadium ions, as reported previously.

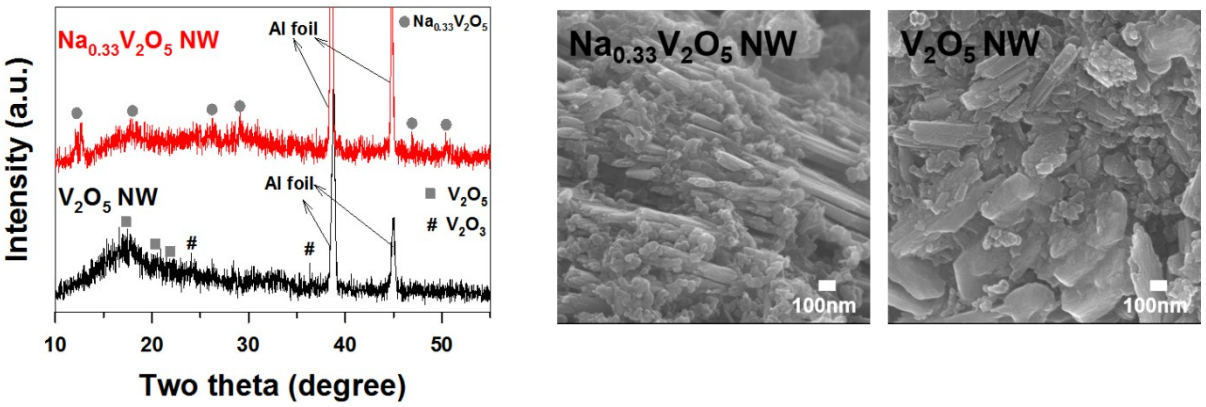

Fig. S5 (Left) X-ray diffraction (XRD) patterns and (right) scanning electron microscopic (SEM) images of $Na_{0.33}V_2O_5$ and V_2O_5 nanowires subjected to the 30th electrochemical cycle.

The effects of electrochemical cycling on the crystal structures and morphologies of the $Na_{0.33}V_2O_5$ and V_2O_5 nanowires are examined with XRD and SEM analyses for their electrochemically-cycled derivatives. As plotted in the left panel of Fig. S5, even after the 30th cycle, the $Na_{0.33}V_2O_5$ nanowire still shows distinct Bragg reflections of layered $Na_{0.33}V_2O_5$ phase with notable intensity depression and peak broadening, indicating the maintenance of its original crystal structure with lowering of crystallinity. In the case of the V_2O_5 nanowire, more prominent amorphization occurs after the electrochemical cycling, suggesting the poor structural stability of the Na-free V_2O_5 nanowire. As can be seen from the right panel of Fig. S5, the SEM analyses for the electrochemically-cycled materials clearly demonstrate that there occur significant decreases in the aspect ratios of 1D nanostructures for both the present materials, although these materials still retain original 1D nanostructured morphologies. In comparison with the V_2O_5 nanowire, the $Na_{0.33}V_2O_5$ one shows a weaker modification of original 1D nanostructure morphology, underscoring the higher morphological stability of sodium vanadate than vanadate. The present findings highlight the higher structural and morphological stability of the $Na_{0.33}V_2O_5$ nanowire than the V_2O_5 one, which contributes to the superior electrode activity of the $Na_{0.33}V_2O_5$ nanowire.